Original article

Evaluation of green synthesized silver nanoparticles utilizing freeze dried curcumin nanocrystals against multidrug resistant bacteria, in-vitro and in-vivo study

Abeer S. Hassan[1] , Noha M.S. Abdelazim[2], Ehsan A.B. Hassan[3], Sherein G. Elgendy [3], Niveen G. El-Gindy[4] , Hebatallah M. Hassan*[3]

1- *Department of Pharmaceutics, Faculty of Pharmacy, South Valley University, Qena 83523, Egypt.*
2- *Assiut General Hospital, Assiut, Egypt.*
3- *Department of Medical Microbiology and Immunology, Faculty of Medicine, Assiut University, Assiut 71515, Egypt.*
4- *Department of Industrial Pharmacy, Faculty of Pharmacy, Assiut University, Assiut, Egypt.*

ARTICLE INFO

ABSTRACT

Background: Development of multidrug-resistant (MDR) organisms is becoming a critical clinical problem for the management of numerous bacterial infections. Investigating other antibacterial drugs is urgently needed that are nontoxic and effective by different mechanisms. **Methods:** This study was aimed to develop silver nanoparticles (AgNPs) utilizing a green synthetic approach involving highly solubilized curcumin in freeze dried nanocrystals (CrNC) as a natural flavonoid reducing agent. **Results:** The fabricated silver nanoparticles were typically found to be spherical in shape with particle size distribution in the range of 10–50 nm and zeta potential of -18.3 ± 2.69 mV. UV-Vis spectroscopy presented a characteristic plasmon peak of silver at 410 nm. The minimal inhibitory concentrations (MICs) of the prepared AgNPs against *Staphylococcus aureus* ATCC® 43300™*, *Escherichia coli* ATCC® 8739™*, *Pseudomonas aeruginosa* ATCC® 27853™* and *Klebsiella pneumoniae* ATCC® 33495™* were 7.8, 1.9, 3.9 and 1.9 μg/ml, respectively. The in-vitro cytotoxicity on human lung fibroblast cells demonstrated that green synthesized silver nanoparticles were nontoxic at the MIC. The in-vivo study revealed that AgNPs loaded hydrogel presented an improved antibacterial efficacy and wound healing effect, with normal skin appearance when compared with silver sulfadiazine cream (Dermazin®). **Conclusion:** The present investigation suggests that green synthesized silver nanoparticles are going to be a promising therapeutic nontoxic antibacterial agent against MDR bacteria with improved wound healing efficacy.

Introduction

Multidrug-resistant (MDR) bacterial pathogens' spread presents a serious health risk to the human world with a significant impact on the treatment of numerous infectious diseases [1,2]. This may be attributed to antibiotic overuse, as well as production of biofilm by a microbial population and ineffective treatment [3]. Methicillin-resistant *Staphylococcus aureus, Escherichia coli, Pseudomonas aeruginosa* and *Klebsiella pneumoniae* are the most frequently seen problematic MDR organisms which cause infections in humans [4].

Silver is a well-known antibacterial therapeutic agent which is highly effective against different types of bacteria, including some types resistant to antibiotics [5]. Silver nanoparticles (AgNPs) have a wide range of antibacterial action against both Gram-positive and Gram-negative microorganisms, restricted bacterial resistance, and relatively low toxicity. AgNPs lead to bacterial death via increasing the permeability of bacterial membrane, penetrating into the cytoplasm, denaturing bacterial proteins, and interfering with DNA replication [6]. These activities are because of the unique characteristics of nanoparticles such as small particle size, particle morphology and large surface area. Green synthesis of AgNPs is an alternative technique for conventional physicochemical approaches that has important benefits, such as safety, environmental eco-friendly, and economical availability, when compared with chemical and physical synthesis techniques [7]. Among the phytochemical natural materials, curcumin (Cr) has attracted significant interest. It has been shown to have antibacterial, anticancer, antiviral, antioxidant, and anti-inflammatory activities [2]. Thus, utilization of curcumin nanocrystals (CrNC) may improve water solubility, increase the theoretical yield of Cr and decrease the hazards of the organic solvents in the process of AgNPs green synthesis [8].

Materials and Methods

Ethical approval

This study was approved by Local Ethics Committee in the Faculty of Medicine, Assiut University, Assiut, Egypt and conducted in accordance with the provisions of the Declaration of Helsinki involving human subjects and animal experiments (Approval No. 17101414).

Materials and reagents

Cr (purity > 95%) was obtained from SD Fine-Chem limited Mumbai India. Silver nitrate and PluronicF-68 were purchased from Sigma-Aldrich (St. Louis, MO, USA). Hydroxypropyl methylcellulose (HPMC), was purchased from United Company for Chem. and Med. Prep., Egypt. Mammalian cell lines: WI-38 (Normal human Lung Fibroblast Cells) were obtained from the American Type Culture Collection (ATCC, Rockville, MD). The cells were transplanted onto RPMI-1640 media with 10% inactivated fetal calf serum and 50 g/ml gentamicin.

Bacterial strains

Staphylococcus aureus ATCC® 43300™*(mecA positive, SCCmec type II positive and methicillin and oxacillin resistant), *Escherichia coli* ATCC® 8739™*, *Pseudomonas aeruginosa* ATCC® 27853™*(contained inducible AmpC beta lactamase), *Klebsiella pneumoniae* ATCC® 33495™* were obtained from American type culture collection (ATCC) from a microbiologic company (USA).

Preparation of curcumin nanocrystals (CrNCs)

Curcumin nanosuspension was prepared using antisolvent nanoprecipitation–ultrasonication method using Pluronic F-68 as stabilizer at concentration of 1 and 2% w/w [9,10].

Characterization of curcumin nanocrystals (CrNCs)

Measurement of curcumin entrapment efficiency percentage

By using an indirect method, the prepared formulation's percentage of entrapment efficiency was calculated by measuring free unentrapped curcumin [11].

Measurement of particle size and zeta potential of CrNCs

Mean particle size (nm) and polydispersity index (PDI) were measured utilizing dynamic light scattering method with a Zetasizer Nano ZS® instrument (Malvern Instruments, Malvern, UK)°. The zeta potential values were found using laser doppler anemometry [12].

Green synthesis of AgNPs using CrNCs

A novel green chemistry synthesis technique was displayed for AgNPs fabrication by reducing silver nitrate (AgNO3) using an aqueous solution of freeze-dried CrNCs [13].

Characterization of green synthesized AgNPs (CrNCs-AgNPs)

Measurement of silver by inductively coupled plasma atomic emission spectroscopy

The concentration of silver was assessed using a Thermo Scientific ICAP 6200 DV inductively coupled plasma–optical emission spectrometer (ICP-OES) [14,15].

UV–visible spectrophotometry analysis of (CrNCs-AgNPs)

The reduction of AgNO3 solution and synthesis of AgNPs using CrNC solution was

monitored by scanning the resulted suspension using a Ultraviolet–Visible (UV–Vis) spectroscopy (Thermo Scientific Evolution™ 300 UV–Vis Spectrophotometer; Thermo Fisher Scientific, Waltham, MA, USA) [15].

Transmission electron microscopy (TEM) observations

A TEM micrograph of the AgNPs was obtained using the JEOL TEM (Model 100 CX II; Tokyo, Japan) [8].

Particle size and zeta potential measurements of (CrNCs-AgNPs)

Dynamic light scattering was utilized to measure mean particle size (nm) and polydispersity index (PDI) with a Zetasizer Nano ZS ® instrument (Malvern Instruments, Malvern, UK). Also, the zeta-potential values were determined by a Malvern Zetasizer Nanoseries ZS ® instrument using laser doppler anemometry [12].

X-ray diffraction (X-RD) analysis

Crystallin feature of the developed AgNPs synthesized using CrNCs was noticed exhibiting a Philips X-ray diffractometer, model PW 1710 (Amsterdam, Netherlands), with CuK radiation (= 1.5405), at voltage of 40 kV and current of 30 mA that were applied for the operation [10].

Fourier-transform infrared analysis(FT-IR)

FT-IR spectra of Cr, CrNCs, synthesized AgNPs powders were recorded employing Shimadzu IR-470 spectrophotometer (Shimadzu, Seisakusho Ltd, Kyoto, Japan) [16].

In-vitro antimicrobial susceptibility testing

Well diffusion method (Agar cup diffusion method)

The antimicrobial activity was assessed for AgNPs prepared using CrNCs as reducing agents (CrNC-AgNPs) and compared with those prepared using free Cr (Cr-AgNPs) against the bacterial strains [17].

Disc diffusion method (kirby-Bauer method) in accordance with CLSI [18].

The suspension's turbidity was adjusted to a bacterial density of 1.5 X 10^8 CFU/ml or 0.5 mcFarland, The appropriate antimicrobial-impregnated discs (filter paper 8 mm, Whatman no. 3, impregnated for 2-3 hours for antibiotic disc) were applied to the agar's surface one at a time. 2µg/ml vancomycin and 2.5µg/ml gentamicin used as positive control [19].

Broth microdilution approach to determine the MIC according to CLSI [18,20].

The antibacterial activity of the different types of AgNPs compared by determining the minimal inhibitory concentration (MIC) against several bacterial strains. Serial two-fold dilutions of each of AgNPs in concentration from 1000 to 0.9 µg/ml were put into a 96-well plastic microdilution tray. Inoculum was prepared by growing reference strains for 24 h in MH broth.

Time kill curve (Effect of CrNC-AgNPs on microbial growth kinetics)

The growth kinetics were studied of bacterial strains in the presence and absence of different concentrations of CrNC-AgNPs using the 96-well plate. Plots of each culture's growth curve at varied nanoparticle concentrations were made [4,21].

In-vitro cytotoxicity assay

The cytotoxic effects of CrNC-AgNPs were tested on WI-38 cell lines (normal human lung fibroblast cells). The cells were cultured in 96-well plates and incubated for 24 hours. Then, different concentrations of CrNC-AgNPs were added to separate wells (three replicates). After 48 hours of further incubation, the number of viable cells was determined using the MTT assay. The optical density of treated and untreated cells was measured using a microplate reader. Cell viability was calculated as a percentage using the formula: % viability = (ODt/ODc) x 100%. ODt represents the mean optical density of wells treated with the test sample, and ODc represents the mean optical density of untreated cells. The Graphpad Prism software was used to calculate the cytotoxic concentration (CC50) using the dose-response curve [22,23].

Preparation of CrNC-AgNPs hydrogel formulation:

In order to facilitate the topical application of AgNs dispersion, hydrogel preparation was fabricated using hydroxypropyl methylcellulose (HPMC15000) as gelling polymer [24].

The developed AgNPs hydrogel formulation (10 g) was evaluated visually for its color and homogeneity and its viscosity was measured utilizing a Brookfield DV-III ULTRA programmable rheometer, model RV, T-bar with number of spindle 96 (Brookfield Engineering Laboratories, Inc., Middleboro, MA, USA) [24].

In-vivo antibacterial activity

Twenty-five mature female mice were purchased from the Faculty of Veterinary Medicine, Assiut University, Egypt. Two doses 150 mg/kg then 100 mg/kg of cyclophosphamide were intraperitoneally administered into mice four days and one day before infection [25]. Skin wounds were made in a 1 cm^2 area without damaging the dermis on the dorsal surfaces of mice using the abrasion method. Five minutes following the wound, each specified region was inoculated with an aliquot of MRSA (*Staphylococcus aureus* ATCC® 43300™*) suspension (100µl of 10^8CFU/mL in phosphate-buffered saline) using a micropipette tip. One day after infection, the animals were separated into five groups of five each, and each group was given the specified treatment (0.5 g/d for 10 d). Group I was the control (without any application), Group II received the blank hydrogel formulation (hydrogel without drugs), Group III received the marketed silver cream (1%) (Dermazin®), group IV was treated with the fabricated CrNCs, and group V was treated with the fabricated CrNC-AgNPs hydrogel (equivalent to 0.1% of silver). One day (before treatment), three days (d), six days (d), nine days (d), and eleven days (d) after infection, swab samples were taken from the surface of the crossing scratches. MRSA (CFU/mL) were counted following serial dilution of the bacterial swab and cultivation on mannitol salt agar, which was then incubated for 24 hours at 37°C.

The wound area of each animal was calculated on the first day of the experiment, and at days 3, 6, 9 and 11 of post wounding using the ruler daily. The percentage % of wound contraction was calculated using the following equation:

$$\text{Percentage \% of wound contraction} = \frac{Wound\ area\ in\ the\ first\ day - Wound\ area\ in\ day\ x}{Wound\ area\ in\ the\ first\ day} \times 100$$

[25,26,27,28].

Histopathological examinations:

Intercellular and intracellular edema of the epidermis, cutaneous edema, and inflammation were assessed in skin sections stained by H&E investigated under a light microscope and photographed. Harris's hematoxylin and eosin was used to produce and stain thin (5 m) paraffin slices [25,26,27,28].

Statistical analysis

All the measurements were conducted in triplicates and results were recorded as means± standard deviations (SD). The data was analyzed using one-way analysis of variance (ANOVA) followed by student t test. For tests, * p < 0.05 was considered to be moderate significant, ** p-value < 0.01 was considered to be strong significant and *** p-value < 0.001 was considered to be very strong significant.

Results

Preparation of CrNCs

Table 1 shows that Cr-NC2 containing 2% of Pluronic F-68 exhibited significant (p < 0.05) smaller particle size and higher value of surface charge (zeta potential). So, it was selected for the development of AgNPs via the green chemistry method.

Fabrication of CrNC-AgNPs

AgNPs were developed using stabilized aqueous solution of CrNCs (containing highly soluble flavonoid curcumin) as reducing agent. The development of AgNPs was adopted by visual monitoring of color changes from yellow color to brown colloidal dispersion. The concentration of AgNPs (1000µg/ml) stock colloidal solution was measured using an inductively coupled plasma–optical emission spectrometer (ICP-OES).

Characterization of green synthesized CrNC-AgNPs

UV-visible spectrophotometry

The aqueous CrNCs showed maximum absorbance at wavelength (λmax) of 440 nm, while the colloidal dispersion of synthesized CrNC-AgNPs showed λmax around 400 nm at different time periods (0.5, 1 and 2h) after the production of colloidal dispersion.

Particle size and zeta potential of CrNC-AgNPs

The mean particle size was found to be of 52.37 ± 1.03 nm. Also, AgNPs dispersion showed a good monodispersity, suitable polydispersity index (PDI) (0.34 ± 0.063) and high value of zeta potential (-18.3 ± 2.69 mV) (**Table1**) which reveals the stability of colloidal dispersion.

X-ray diffraction analysis

X- ray analysis was performed to confirm crystallin structure of the produced AgNPs using CrNCs as a phytochemical reducing agent. The spectrum of synthesized AgNPs demonstrated diffraction peaks at 38.92°, 44.26°, 64.54° and 77.32°. Also, the diffraction of Cr-NC revealed the disappearance of characteristic diffraction peaks of pure crystallin Cr (**Figure 1).**

The FTIR study

The spectra of CrNCs and synthesized AgNPs using CrNCs. The spectrum of AgNPs showed strong peaks at 3370, 2920 and around 1640, corresponding to the functional groups of amide C=O (around 1640 cm−1), C-H stretch (around 2920 cm−1) and O-H vibration stretch (around 3370 cm−1). The FTIR result illustrates that the freeze-dried CrNCs does not produce any new absorption peak after silver reduction. The spectrum of the NCs represents no characteristic bands of pure Cr, proving that Cr changed to amorphous form (in agreement with X-ray results).

Transmission electron microscopy (TEM)observations

The images of TEM and the histogram of AgNPs that developed utilizing CrNCs as reducing agent is presented in (**Figure 2 a and b**). **Figure 1. (A):** XRD patterns of AgNPs prepared using CrNC as reducing agent, freeze dried CrNC and Free Cr. (**B**): FTIR spectra of AgNPs synthesized using CrNC as reducing agent, freeze dried CrNC and Free Cr. **Figure 2.** TEM micrographs (a) and particle size distribution histogram (b) of AgNPs synthesized using CrNC as reducing agent.

In-vitro antimicrobial susceptibility testing

Well diffusion method (Agar cup diffusion method)

All the bacterial strains that were examined had distinct inhibition zones after being exposed to 1000 ‑ to 1.9 µg/mL of AgNPs (**Table 2**).

Disc diffusion method (kirby-Bauer method)

At concentration of 1000 µg/ml CrNC-AgNPs formulation was more effective than Cr-AgNPs against *Staphylococcus aureus* ATCC® 43300™*, *Escherichia coli* ATCC® 8739™*, *Pseudomonas aeruginosa* ATCC® 27853™* and *Klebsiella pneumoniae* ATCC® 33495™* with a zone of inhibition of 19.3, 15, 15.3, 16.3mm, respectively. The results show that the CrNC-AgNPs exhibited an improved antibacterial effect against all bacterial strains in dose dependent manner (**Table 3**). Effect of CrNC-AgNP was more than effect of vancomycin against *Staphylococcus aureus* ATCC® 43300™*, and more than effect of gentamicin against *Escherichia coli* ATCC® 8739™*, and more than effect of gentamicin against *Pseudomonas aeruginosa* ATCC® 27853™* and less than effect of gentamicin against *Klebsiella pneumoniae* ATCC® 33495™* (**Table 4).**

Broth microdilution method (MIC, MBC)

The results of antibacterial activity studies illustrated that the developed CrNC-AgNPs shows a broad-spectrum inhibitory effect against all tested strains. *Staphylococcus aureus* ATCC® 43300™* was found to be the most resistant among the tested strains with an MIC value of 7.8 µg/ml. *Escherichia coli* ATCC® 8739™* and *Klebsiella pneumoniae* ATCC® 33495™* were found to be most sensitive among the examined strains with an MIC value of 1.9 and 1.9 µg/ml (**Table 5**).

Time kill curve (Performance of CrNC-AgNPs on microbial growth kinetics)

The growth kinetics of bacterial strains in the presence and absence of different concentrations of CrNC-AgNPs were studied (**Figure 3**).

In-vitro cytotoxicity assay

Cell viability analysis exhibited that exposure of the human fibroblasts to different concentrations of CrNC-AgNPs (the highest MIC value), did not produce any effects on the viability of the normal cells comparing with untreated control cells, proving that the prepared AgNPs are nontoxic and biocompatible (**Table 6**). The MTT assay was conducted after 48h of incubation of fibroblast normal cells with CrNC-AgNPs at concentrations ranged from 1 up to 500 µg/ml which include MIC values (7.8, 1.9, 3.9 and 1.9 µg/ml) of CrNC-AgNPs against *Staphylococcus aureus* ATCC® 43300™*, *Escherichia coli* ATCC® 8739™*, *Pseudomonas aeruginosa* ATCC® 27853™* and *Klebsiella pneumoniae* ATCC® 33495™*, respectively.

Figure 3. Growth kinetic curve of *Staphylococcus aureus* ATCC® 43300™* , *Escherichia coli* ATCC® 8739™*, *Pseudomonas aeruginosa* ATCC® 27853™* and *Klebsiella pneumoniae* ATCC® 33495™* in the presence and absence of different concentrations of CrNC-AgNPs.

In-vivo antibacterial activity

Using female mice, the wound-healing performance of CrNC and CrNC-AgNPs was assessed. Representative mouse skin attrition wounds were photographed each day at varied intervals in all the study groups (**Figure 4).** Comparing the groups who got marketed silver cream and CrNC-AgNPs gel, the group that received the latter showed a better efficiency in the healing of the contaminated area (**Figure 5**). Both mice treated

with blank gel and untreated animals bled pus from their infected lesions. The mouse groups had an average bacterial count of around 4×10^6 CFU/mL before the therapy (1 day) began (**Figure 6**) displays the percentages of bacterial count in mice skin abrasions (n=5) at different time intervals after daily application of the topical treatment (as opposed to the untreated control group). The mice group receiving CrNC-AgNPs hydrogel demonstrated a significantly (P <0.001) quicker and better decrease in bacterial growth than the other groups over the course of the 11-day treatment period. The skin treated with CrNC-AgNPs hydrogel showed 18% of the bacterial count in the control untreated skin in the first bacterial swab assay after the commencement of the therapy, compared to 33.5% and 92% for the groups that received marketed silver cream (Dermazin®) and blank hydrogel, respectively (3d). In the most recent bacterial swab evaluation (11d), the skin treated with CrNC-AgNPs hydrogel revealed 1.3% of the bacterial count in the control untreated skin, whereas the groups that treated with CrNC hydrogel, marketed silver cream (Dermazin®) and blank hydrogel exhibited 21, 20 and 50 percent of the bacterial count, respectively, in the control untreated skin and in comparison to the mice group that received marketed silver cream (Dermazin®) and CrNC hydrogel, the CrNC-AgNPs hydrogel group significantly (P <0.001) reduced bacterial growth more quickly and effectively. The CrNC-AgNPs hydrogel treated mice group demonstrated a significantly (P <0.001) quicker and superior reduction in bacterial growth than the group control, which was very significant.

Histological examination

The H&E stained sections of wounded areas of all groups were examined to evaluate the histological features of healing rates in each group. It was observed that compared to lack of complete epithelization, presence of surface exudate and shredded cells mixed with bacterial aggregation with features of inflammatory cells in the wound base (wounded untreated) (G1). The treated groups (medicinal medication and CrNC hydrogel) (G3, G4) showed complete but hyperplastic surface epithelization and decreased inflammatory reactions in the wound base. In the group treated with CrNC-AgNPs (G5), thin epithelization; nearly similar to control, was observed. The wound base showed normal collagen and fibroblasts and absence of inflammatory cells. Primordial hair follicles as a feature of hair growth could be observed in the wounded area treated with CrNC-AgNPs (**Figure 7**).

Figure 4. A series of images over time of MRSA-infected skin abrasion wounds on representative mice. First group as control (untreated), second group treated with blank hydrogel, third group treated with commercial silver (1%) (Dermazin®), fourth group treated with CrNC gel and fifth group treated with CrNC-AgNPs hydrogel (0.1%). **Figure 5.** Percentages of the wound contraction in the examined different groups: First group as control (untreated), second group treated with blank hydrogel, third group treated with commercial silver (1%) (Dermazin®) and fourth group treated with CrNC-AgNPs hydrogel (0.1%) in days 1, 3, 6, 9 and 11. **Figure 6.** Bacterial counts expressed as a proportion of the bacterial counts in the control, untreated mice group were found in the infected scratch wounds of several mouse groups at various time points. First group as control (untreated), second group treated with blank hydrogel, third group treated with commercial silver (1%) (Dermazin®) and fourth group treated with CrNC-AgNPs hydrogel (0.1%).

Figure 7. Gross picture to wounded area in different groups to show the healing rate, notice the most response is in treated groups (D, E) with most effective in group E (CrNC-AgNPs).

Table 1. Characterization of the fabricated AgNPs and CrNCs dispersions for particle size, PDI and zeta potential

Formulation	Particle size	PDI	Zeta potential
Cr-NC1*	201.13 ± 21.87	0.29 ± 0.049	-4.95 ± 1.60
Cr-NC2#	196.03 ± 2.31	0.28 ± 0.026	-17.46 ± 1.31
G-AgNPs**	52.37 ± 1.03	0.34 ± 0.063	-18.3 ± 2.69
C-AgNPs ##	46.56 ± 6.20	0.30 ± 0.087	-19.06 ± 2.86

*Curcumin Nanocrystals contains Pluronic F-68 as stabilizer 1%w/v
Curcumin Nanocrystals contains Pluronic F-68 as stabilizer 2 %w/v
** Silver nanoparticles fabricated by green synthesis using Cr-NC
Silver nanoparticles as a control

Table 2. Evaluation of antibacterial activity of different concentrations of Cr-AgNPs and CrNC-AgNPs against *Staphylococcus aureus* ATCC® 43300™*, *Escherichia coli* ATCC® 8739™*, *Pseudomonas aeruginosa* ATCC® 27853™* and *Klebsiella pneumoniae* ATCC® 33495™* by agar well diffusion

Microorganism	Conc. Of antimicrobial agent (µg/ml)	Mean of Zone diameter of Cr-AgNPs ± SD (mm) (n=3)	Mean of Zone diameter of CrNC-AgNPs ± SD (mm) (n=3)	p.value
Staphylococcus aureus ATCC® 43300™*	1000	19.3± 0.7	24.3± 0.6	< 0.001
	500	18± 0.5	23± 0.7	< 0.001
	250	16.6± 0.5	22± 0.5	< 0.001
	125	14.6± 0.6	21± 0.6	< 0.001
	62.5	11.6± 0.7	20.3± 0.8	< 0.001
	31.2	0	18.3± 0.2	< 0.001
	15	0	19.6± 0.5	< 0.001
	7.8	0	17 ± 0.4	< 0.001
	3.9	0	0	
	1.9	0	0	
Escherichia coli ATCC® 8739™*	1000	18.6± 0.4	22.6± 0.2	< 0.001
	500	17.6± 0.5	22± 0.3	< 0.01
	250	17± 0.4	20.6± 1	< 0.001
	125	14.3± 0.4	20.3± 0.5	< 0.001
	62.5	0	19± 1	< 0.001
	31.2	0	18.6± 0.5	< 0.001
	15	0	17.6± 0.8	< 0.001
	7.8	0	15.3± 0.7	< 0.001
	3.9	0	12± 0.6	< 0.001
	1.9	0	10± 0.5	< 0.001
Pseudomonas aeruginosa ATCC® 27853™*	1000	17.3± 0.3	24.3± 0.3	< 0.001
	500	15.6± 0.4	21.6± 0.1	< 0.001
	250	15.1± 0.6	19.3± 0.6	< 0.001
	125	12.3± 0.5	18.6± 0.5	< 0.001
	62.5	0	18.3± 0.3	< 0.001
	31.2	0	17.3± 0.4	< 0.001
	15	0	17.3± 0.5	< 0.001
	7.8	0	17± 0.3	< 0.001
	3.9	0	17± 0.3	< 0.001
	1.9	0	4.6± 0.6	< 0.001
Klebsiella pneumoniae ATCC® 33495™*	1000	16.6± 0.4	22.3± 0.8	< 0.001
	500	15.6± 1	20.3± 0.5	< 0.01
	250	15± 1	20± 0.2	< 0.01
	125	14.3± 0.2	20.3± 0.2	< 0.001
	62.5	0	19.3± 0.5	< 0.001
	31.2	0	19± 0.3	< 0.001
	15	0	15± 1	< 0.001
	7.8	0	14± 0.2	< 0.001
	3.9	0	13± 0.4	< 0.001
	1.9	0	10± 0.2	

Note: p-value < 0.01 was considered to be strong significant and p-value < 0.001 was considered to be very strong significant.
Abbreviations: Cr-AgNPs silver nanoparticles prepared using free curcumin, **CrNC-AgNPs** silver nanoparticles prepared using freeze dried curcumin nanocrystal, **SD** standard deviation.

Table 3. Evaluation of antibacterial activity of different concentrations of Cr-AgNPs and CrNC-AgNPs against *Staphylococcus aureus* ATCC® 43300™*, *Escherichia coli* ATCC® 8739™*, *Pseudomonas aeruginosa* ATCC® 27853™* and *Klebsiella pneumoniae* ATCC® 33495™* by agar disc diffusion

Microorganism	Conc. Of antimicrobial agent (μg/ml)	Mean of Zone diameter of Cr-AgNPs ± SD (mm) (n=3)	Mean of Zone diameter of CrNC-AgNPs ± SD (mm) (n=3)	p.value
Staphylococcus aureus ATCC® 43300™*	1000	15±	19.3±	< 0.001
	500	14± 1	17± 0.5	< 0.01
	250	12.3± 0.2	14± 0.5	< 0.01
	125	0	7± 1	< 0.001
	62.5	0	0	
	31.2	0	0	
	15	0	0	
	7.8	0	0	
	3.9	0	0	
	1.9	0	0	
Escherichia coli ATCC® 8739™*	1000	12± 0.7	15± 0.2	< 0.01
	500	10.6± 0.5	14± 0.6	< 0.01
	250	0	12.3± 0.7	< 0.001
	125	0	11.3± 0.3	< 0.001
	62.5	0	0	
	31.2	0	0	
	15	0	0	
	7.8	0	0	
	3.9	0	0	
	1.9	0	0	
Pseudomonas aeruginosa ATCC® 27853™*	1000	11.3± 0.4	15.3± 0.3	< 0.01
	500	7± 0.4	14.3± 0.1	< 0.001
	250	0	13.3± 0.4	< 0.001
	125	0	11± 0.5	< 0.001
	62.5	0	0	
	31.2	0	0	
	15	0	0	
	7.8	0	0	
	3.9	0	0	
	1.9	0	0	
Klebsiella pneumoniae ATCC® 33495™*	1000	12± 0.1	16.3± 0.2	< 0.001
	500	11.3± 0.6	16± 0.8	< 0.01
	250	10.6± 1	15.3± 0.6	< 0.01
	125	0	14 ± 0.5	< 0.001
	62.5	0	10± 0.5	< 0.001
	31.2	0	0	
	15	0	0	
	7.8	0	0	
	3.9	0	0	
	1.9	0	0	

Note: p-value < 0.01 was considered to be strong significant and p-value < 0.001 was considered to be very strong significant.
Abbreviations: Cr-AgNPs silver nanoparticles prepared using free curcumin, **CrNC-AgNPs** silver nanoparticles prepared using freeze dried curcumin nanocrystal, **SD** standard deviation

Table 4. Comparison between antibacterial effect of CrNC and CrNC-AgNPs with antibiotics effect

Microorganism	Zone of inhibition ± SD (mm) (n=3)					p.value 1 (CrNC and antibiotic)	p.value 2 (CrNC-AgNPs and antibiotic)
	Blank	Free-Cr	AB (2µg/ml vancomycin and 2.5µg/ml gentamicin)	CrNC	CrNC-AgNP		
Staphylococcus aureus ATCC® 43300™*	0	10	19 ±1	17.8 ±0.8	20 ±1	(p>0.05)	(p > 0.05)
Escherichia coli ATCC® 8739™*	0	12	17 ±0.7	18 ±0.4	18 ±0.5	(p>0.05)	(p > 0.05)
Pseudomonas aeruginosa ATCC® 27853™*	0	11.5	18 ±0.5	18 ±0.4	20 ±1	(p>0.05)	**(p < 0.05)**
Klebsiella pneumoniae ATCC® 33495™*	0	11	17 ±0.5	16 ± 1	17 ±2	(p>0.05)	(p > 0.05)

Note: * p < 0.05 was considered to be moderate significant,
Abbreviations: CrNC curcumin nanocrystal, **CrNC-AgNPs** silver nanoparticles prepared using freeze dried curcumin nanocrystal, **SD** standard deviation.
Vancomycin for *Staphylococcus aureus* ATCC® 43300™*
Gentamicin *for Escherichia coli* ATCC® 8739™*, *Pseudomonas aeruginosa* ATCC® 27853™* and *Klebsiella pneumoniae* ATCC® 33495™*

Table 5. Broth microdilution method used to determine MIC and MBC of Cr-AgNPs and CrNC-AgNPs dispersions against *Staphylococcus aureus* ATCC® 43300™*, *Escherichia coli* ATCC® 8739™*, *Pseudomonas aeruginosa* ATCC® 27853™* and *Klebsiella pneumoniae* ATCC® 33495™*

Antimicrobial agent	MIC µg/ml				MBC µg/ml			
	Staphylococcus aureus ATCC® 43300™*	*Escherichia coli* ATCC® 8739™*	*Pseudomonas aeruginosa* ATCC® 27853™*	*Klebsiella pneumoniae* ATCC® 33495™*	*Staphylococcus aureus* ATCC® 43300™*	*Escherichia coli* ATCC® 8739™*	*Pseudomonas aeruginosa* ATCC® 27853™*	*Klebsiella pneumoniae* ATCC® 33495™*
Cr-AgNPs	125	125	250	250	125	250	250	500
CrNC-AgNP	7.8	1.9	3.9	1.9	7.8	1.9	3.9	3.9
p.value	P < 0.001	P <0.001	P < 0.001	P < 0.001	P < 0.001	P < 0.001	P < 0.001	P < 0.001

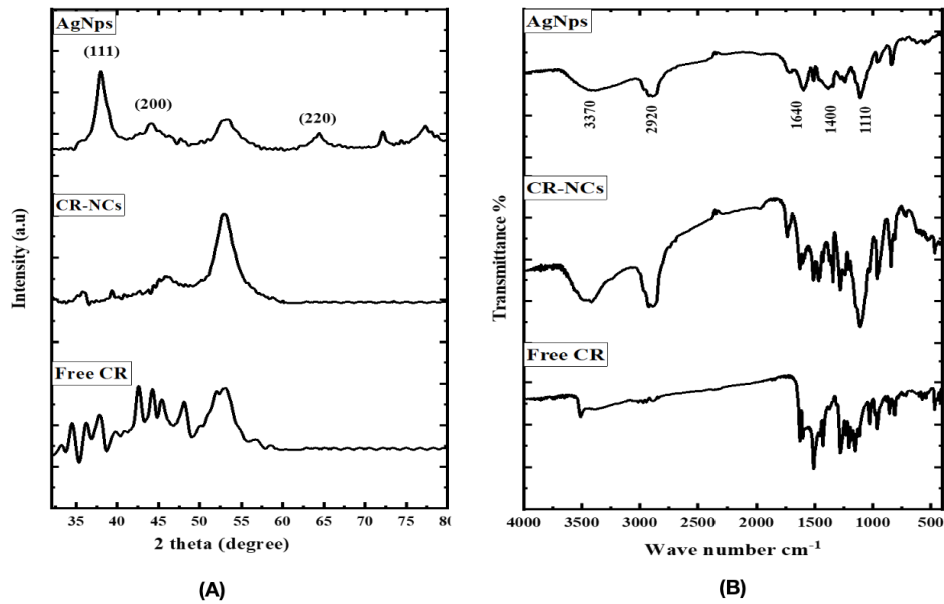**Note**: p-value < 0.001 was considered to be very strong significant.
Abbreviations: Cr-AgNPs silver nanoparticles prepared using free curcumin, **CrNC-AgNPs** silver nanoparticles prepared using freeze dried curcumin nanocrystal.

Table 6. Cytotoxicity test of CrNC-AgNPs using human lung fibroblast normal cells
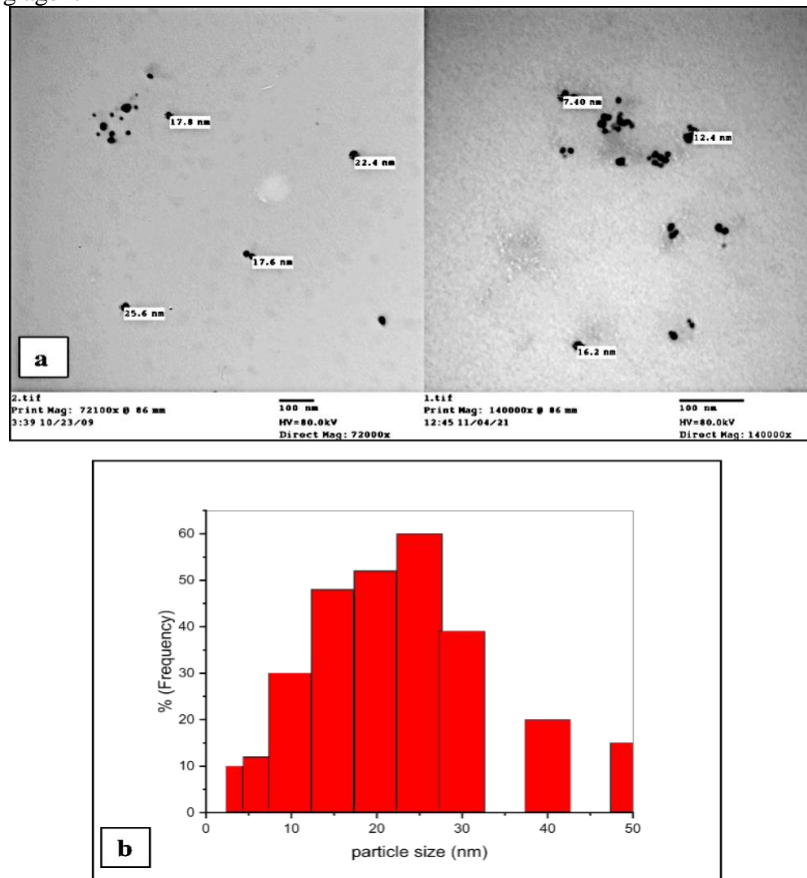
Sample conc. (µg/ml)	Viability %	Inhibitory %	S.D. (±)
500	5.97	94.03	0.51
250	15.28	84.72	0.96
125	37.52	62.48	1.74
62.5	56.04	43.96	2.18
31.25	79.13	20.87	1.59
15.6	92.38	7.62	0.64
7.8	**97.16**	**2.84**	0.82
3.9	**100**	**0**	
2	100	0	
1	100	0	
0	100	0	

Note: MICs of CrNC-AgNPs against *Staphylococcus aureus* ATCC® 43300™*, *Escherichia coli* ATCC® 8739™*, *Pseudomonas aeruginosa* ATCC® 27853™* and *Klebsiella pneumoniae* ATCC® 33495™* were 7.8, 1.9, 3.9 and 1.9 respectively

Figure 1. (A): XRD patterns of AgNPs prepared using Cr-NC as reducing agent, Freeze dried Cr-NC and Free Cr. (B): FTIR spectra of AgNPs synthesized using Cr-NC as reducing agent, freeze dried Cr-NC and Free Cr. Origin-2018 software was used to prepare this graph
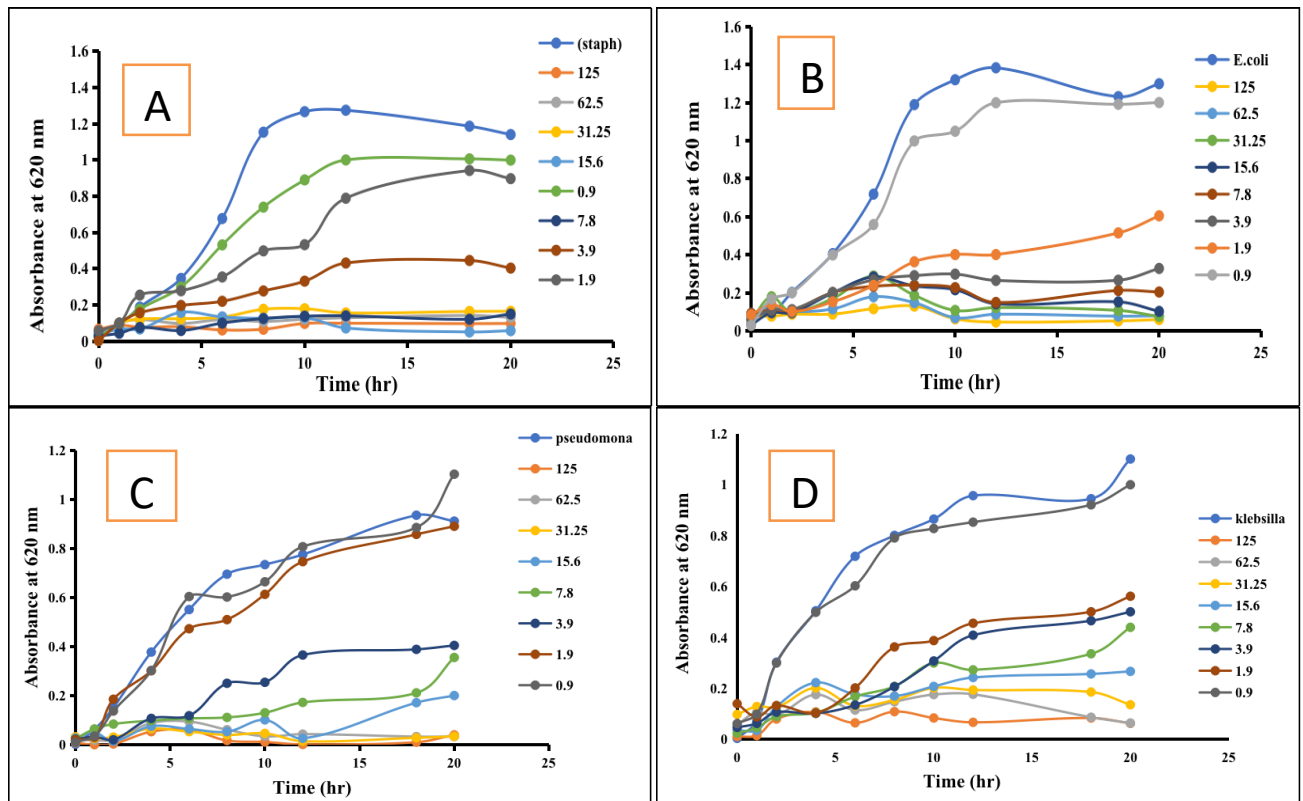

(A)

(B)

Figure 2. TEM micrographs (a) and particle size distribution histogram (b) of AgNPs synthesized using Cr-NC as reducing agent

Abbreviations: AgNP: silver nanoparticles, Cr-NC: curcumin nanocrystals, TEM: transmission electron microscopy, Cr: curcumin

Figure 3. Growth kinetics curve of *Staphylococcus aureus (A), Escherichia coli(B), Pseudomonas aeruginosa(C)* and *Klebsiella pneumoniae(D)* in presence and absence of different concentrations of CrNC-AgNPs
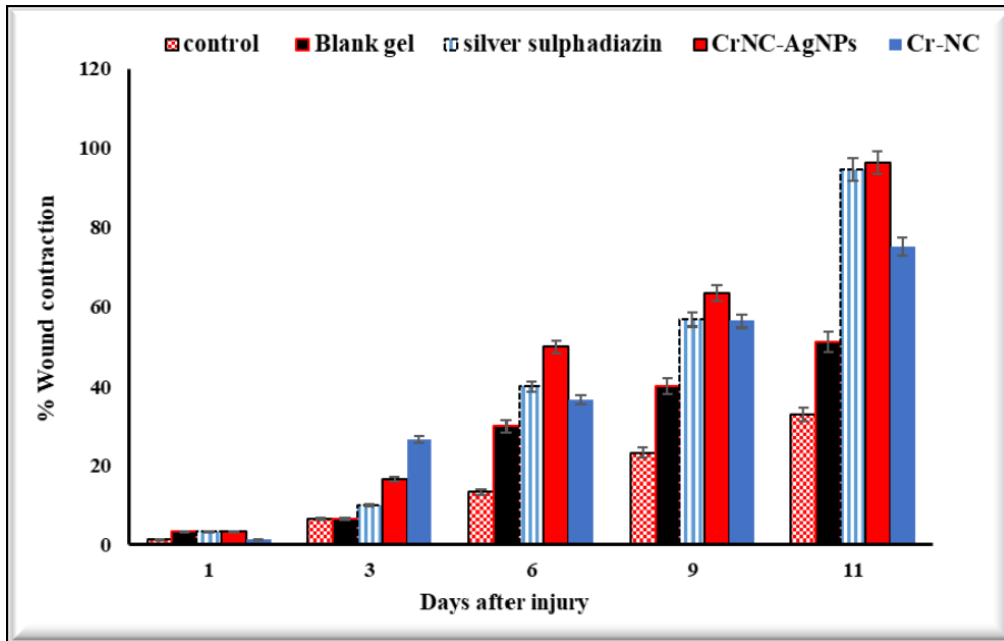

Figure 4. A series of images over time of MRSA-infected skin abrasion wounds on representative mice. First group as control G1(untreated), second group G2 (treated with blank hydrogel), third group G3 (treated with commercial silver sulfadiazine (1%)), fourth group G4 (treated with Cr-NC gel) and fifth G5 group (treated with CrNC-AgNPs hydrogel (0.1%)) .
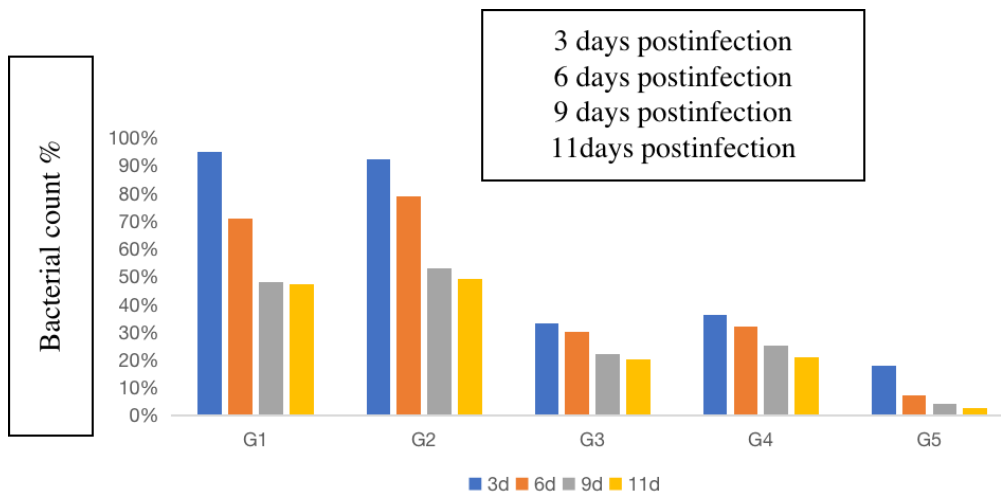

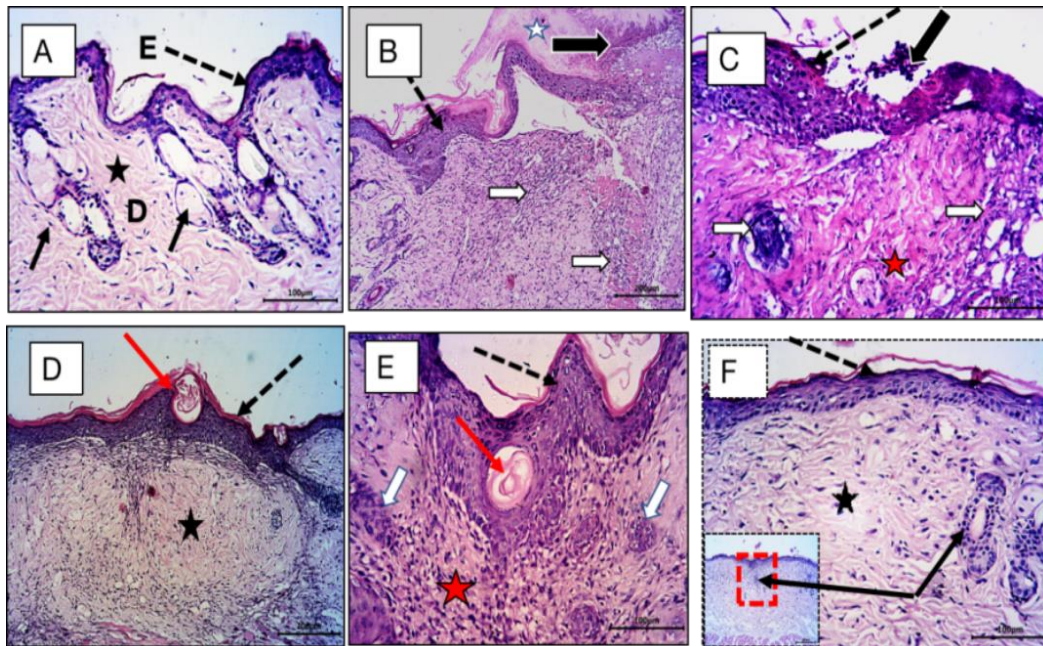Abbreviation: MRSA: methicillin-resistant *Staphylococcus aureus*, AgNPs: silver nanoparticles

Figure 5. Percentages of the wound contraction in four different groups: First group as control (untreated), second group (treated with blank hydrogel), third group (treated with commercial silver sulfadiazine (1%)), fourth group (treated with CR-NC (1 %) hydrogel) and fifth group (treated with CrNC-AgNPs hydrogel (0.1%)) in days 1, 3, 6, 9 and 11

Figure 6. Bacterial counts expressed as a proportion of the bacterial counts in the control, untreated mice group were found in the infected abrasion wounds of several mouse groups at various time points. First group as control (untreated), second group (treated with blank hydrogel), third group (treated with commercial silver sulfadiazine (1%)) and fourth group (treated with CrNC-AgNPs hydrogel (0.1%)).

Figure 7. Gross picture to wounded area in different groups to show the healing rate notice the most response is in treated groups (D,E) with most effective in group E (CrNC-AgNPs).

Discussion

Curcumin was formulated as freeze-dried nanocrystals with Pluronic F-68 as a stabilizer at a concentration of 2%w/v. These nanocrystals were used as a reducing agent to develop AgNPs through green synthesis [29]. The synthesized AgNPs have desirable characteristics and high acceptable yield which indicate the efficiency of Cr freeze dried nanocrystals to reduce silver nitrate in an aqueous solution forming AgNPs. Therefore, CrNC could be utilized as promising reducing agents for AgNPs fabrication *via* green chemistry approach.

The antibacterial effect of CrNC-AgNPs against the MDR bacterial strains was investigated using the agar well diffusion method. *Pseudomonas aeruginosa* ATCC® 27853TM* was shown to have the highest resistance pattern with a mean minimum inhibition zone of 18.6mm for CrNC-AgNPs at concentration 125 μg/ml. *Staphylococcus aureus* ATCC® 43300™* was found to be most sensitive with a mean maximum inhibition zone of 21mm for CrNC-AgNPs at concentration 125 μg/ml. Qais, Shafiq et al. used Murraya koenigii in synthesis of AgNPs, they found that the most resistant microorganism was methicillin-sensitive *S. aureus* (*MSSA2*)with a minimum inhibition zone of 16mm for MK-AgNPs at 100μg/ml. *E. coli* was found to exhibit a maximum inhibition zone of 21mm [4]. Another study by Hetta, Al-Kadmy et al. used

50μg/ml of AgNPs against two hundred isolates of multidrug resistant *Acinetobacter baumannii*, they found that AgNPs produced inhibition zone in all the previously tested bacterial strains (mean 16mm) [21].

CrNC-AgNPs exhibit broad-spectrum antibacterial activity, surpassing that of Cr-AgNPs. The (MICs) of CrNC-AgNPs against tested bacterial strains were 7.8, 1.9, 3.9, and 1.9 g/mL. for *Staphylococcus aureus* ATCC® 43300™*, *Escherichia coli* ATCC® 8739™*, *Pseudomonas aeruginosa* ATCC® 27853™* and *Klebsiella pneumoniae* ATCC® 33495™*, respectively.

As concluded by Qais, Shafiq et al., the MIC for MK-AgNPs against MRSA was measured to be 32 μg/ml. *E.coli* was found to be most sensitive among the examined strains with an MIC value of 16 μg/ml, while extended-spectrum β-lactamase-producing *E. coli* (*ECESβL*) was found to have high resistance behavior against AgNPs with an MIC value of 64 μg/ml [4]. Similar outcomes have been reported in the past, when AgNPs synthesized utilizing eucalyptus globulus were shown to exhibit MIC and MBC values against *E. coli* of 36 and 42 g/ml [32,33]. Additionally, against methicillin-resistant *S. aureus*, Ansari and Alzohairy investigated MIC and MBC values of AgNPs generated by green synthesis method using phoenix dactylifera seed extracts, and it was found

to be 10.67 and 17.33 g/ml, respectively for MRSA [34] . These differences could be caused by the various inherent tolerance levels of the test strains employed in the analysis, the size and features of the nanoparticles, and the methodologies used for measuring the MIC and MBC.

In similar study, Jaiswal and Mishra, used free Cr in synthesis of AgNPs, they discovered that Cr-AgNPs displayed improved antibacterial activity as seen by MIC values in the range of 2.5–10 mg/L, indicating increased antibacterial efficacy, as opposed to AgNPs manufactured using a chemical synthesis strategy, which showed MIC in the range of 10-15 mg/L. The most susceptible strain was identified as *B. subtilis* ATCC 6633, which also had the lowest MIC (2.5 mg/L), whereas the least susceptible strain was identified as *P. aeruginosa* ATCC 14886, which had the highest MIC (10 mg/L). Intermediate MIC values (5 mg/L) were found for *E. coli* ATCC 25922 and *S. aureus* ATCC 9144 [20].

Qais, Shafiq et al. investigated that the main concept of the enhanced antibacterial activity of AgNPs is related to the synergistic effect between AgNPs and natural herbal products [4]. According to Cardozo et al., the combination of phenazine-1-carboxamide and AgNPs improved the antibacterial efficacy against *MRSA* strains by 32-fold and changed the morphology of bacterial cell walls [35,36].

In the presence of CrNC-AgNPs at different concentrations, the growth curves of the tested strains showed three stages: lag phase, exponential phase, and stabilization phase. No decrease in growth was observed. Without CrNC-AgNPs, the bacteria quickly entered the exponential phase. However, when exposed to concentrations equal to or above the (MIC) of CrNC-AgNPs, the bacteria experienced a delay in growth, which became more pronounced with increasing concentrations. As concluded by Jaiswal and Mishra, when 10^5 CFU/ml bacterial cells were incubated with examined antibacterial compound (Cr-AgNPs, AgNPs, free Cr, AgNO3 and antibiotics), the results showed that the growth rate of bacteria was decreased as compared to the control. Except free Cr, all other samples exhibited complete inhibition after 5–6 h. While, free Cr showed limited growth in all strains but it was not completely inhibited as obtained in the case of using Cr-AgNPs [20].

In this study the biocompatibility of CrNC-AgNPs was examined displaying the normal human lung fibroblast cells , CrNC-AgNPs at concentration of MIC cell viability remained higher than 97%. These observations were in matching with those obtained in previous works, where a significant (p < 0.05) reduction in cell viability was obtained for AgNPs at higher concentrations [37]. Jaiswal and Mishra used the MTT test to determine the preferential toxicity of Cr-AgNPs towards bacterial cells over mammalian cells in human skin keratinocytes [38]. They found that Cr-AgNPs showed cytotoxic concentration on the human normal cells much higher than MIC against bacteria. The selective toxicity of the AgNPs towards bacterial inhibition suggests improved safety of the produced nanoparticles for human cells and is harmful against bacterial cells [39]. They investigated the safe application of AgNPs as antibacterial agents in external wound dressing without harm to skin keratinocytes. In our study, the mice group that received CrNC-AgNPs hydrogel demonstrated a considerably very strong significant (P < .001), faster and superior reduction in bacterial growth as compared with the group treated with the marketed silver cream (Dermazin®). Nearly similar results have been reported by Mekkawy, El-Mokhtar et al., they synthesized AgNPs by silver nitrate biological reduction using extract of the fungus Fusarium verticillioides (green chemistry approach), the mice group received 0.1% AgNPs hydrogel demonstrated quicker and better decrease in bacterial growth over the 15-day treatment period. In the first bacterial swab analysis after starting the therapy, the AgNPs hydrogel-treated skin had a bacterial count of 20.5% of the untreated control skin, compared to 44.7% and 94.5% for the maketed silver cream (Dermazin®) and blank hydrogel treated groups, respectively (3d)[25]. Another study reported wound management applications of AgNPs loaded bacterial cellulose hydrogels. They concluded that these novel dressings showed antimicrobial effects against *Staphylococcus aureus*, *Pseudomonas aeruginosa*, and *Candida auris*, which are the three common wound-infecting pathogenic microorganisms [40].

Conclusion

A green synthesis method used to create AgNPs using Cr and CrNCs as a reducing agent. The resulting CrNC-AgNPs had a spherical shape, were evenly distributed, and had a small size. The synthesized CrNC-AgNPs demonstrated high

antibacterial activity against various bacteria, compared with Cr-AgNPs. The CrNC-AgNPs had low MICs against the bacteria, effectively reducing their growth. The study also developed a hydrogel using the CrNC-AgNP, which showed superior antibacterial and wound healing properties compared to a commercially available silver cream. Overall, the green-synthesized nanoparticles have great potential as non-toxic antibacterial agents with excellent wound healing capabilities.

Financial support and Sponsorship

None

Conflicts of interest

The authors declare that they do not have any conflict of interest.

References

1- Lena P, Karageorgos SA, Loutsiou P, Poupazi A, Lamnisos D, Papageorgis P, et al . Multidrug-Resistant Bacteria on Healthcare Workers' Uniforms in Hospitals and Long-Term Care Facilities in Cyprus. Antibiotics 2022;11(1):49.

2- Ibrahim N B, Hassan E, Elgendy S, Hassan H, Hassan A, El-Gindy N. IN- VITRO EVALUATION OF NANOCURCUMIN AGAINST MULTI-DRUG RESISTANT BACTERIA. Bulletin of Pharmaceutical Sciences Assiut University 2023; 46(1): 433-448.

3- Tang HW, Phapugrangkul P, Fauzi HM, Tan JS. Lactic Acid Bacteria Bacteriocin, an Antimicrobial Peptide Effective Against Multidrug Resistance: a Comprehensive Review. International Journal of Peptide Research and Therapeutics 2022;28(1):1-14.

4- Qais FA, Shafiq A, Khan HM, Husain FM, Khan RA, Alenazi B, et al.**Q4** Antibacterial effect of silver nanoparticles synthesized using Murraya koenigii (L.) against multidrug-resistant pathogens. Bioinorganic chemistry and applications 2019;2019.

5- Barabadi H, Mojab F, Vahidi H, Marashi B, Talank N, Hosseini O, et al.**Q4** Green synthesis, characterization, antibacterial and biofilm inhibitory activity of silver nanoparticles compared to commercial silver nanoparticles. Inorganic Chemistry Communications 2021;129:108647.

6- Yin IX, Zhang J, Zhao IS, Mei ML, Li Q, Chu CH. The antibacterial mechanism of silver nanoparticles and its application in dentistry. International journal of nanomedicine 2020;15:2555.

7- Vishwanath R, and Negi B. Conventional and green methods of synthesis of silver nanoparticles and their antimicrobial properties. Current Research in Green and Sustainable Chemistry 2021;4:100205.

8- Lyu Y, Yu M, Liu Q, Zhang Q, Liu Z, Tian Y, et al. Synthesis of silver nanoparticles using oxidized amylose and combination with curcumin for enhanced antibacterial activity. Carbohydrate polymers 2020;230:115573.

9- Abdelbary AA, Al-Mahallawi AM, Abdelrahim ME, Ali AM. Preparation, optimization, and in vitro simulated inhalation delivery of carvedilol nanoparticles loaded on a coarse carrier intended for pulmonary administration. International journal of nanomedicine 2015;10:6339.

10- Hassan AS, El-Mahdy MM, El-Badry M, El-Gindy GE-DA. Different Approaches for Enhancement of Curcumin Aqueous Solubility and Dissolution rate. Journal of advanced Biomedical and Pharmaceutical Sciences 2019;2(4):152-163.

11- Alam S, Panda JJ, Chauhan VS. Novel dipeptide nanoparticles for effective curcumin delivery. International journal of nanomedicine 2012;7:4207.

12- Aref ZF, Bazeed SEES, Hassan MH, Hassan AS, Ghweil AA, Sayed MAA, et al. Possible Role of Ivermectin Mucoadhesive Nanosuspension Nasal Spray in Recovery of Post-COVID-19 Anosmia. Infection and Drug Resistance 2022:5483-5494.

13- Nagnath JP, Davis D, Ovia P, Swaminathan S, Deepa K. Boltzmann equation for the modelling of formation of silver nanoparticles using trisodium citrate as the reducing agent. Bulletin of Materials Science 2021;44:1-6.

14- Iglesias M, and Torrent L. Silver Nanoparticles and Ionic Silver Separation Using a Cation-Exchange Resin. Variables Affecting Their Separation and Improvements of AgNP Characterization by SP-ICPMS. Nanomaterials 2021;11(10):2626.

15- Ahn E-Y, Jin H, Park Y. Green synthesis and biological activities of silver nanoparticles prepared by Carpesium cernuum extract. Archives of pharmacal research 2019;42(10):926-934.

16- Hassan AS, Soliman GM, El-Mahdy MM, El-Gindy GE-DA. Solubilization and enhancement of ex vivo vaginal delivery of progesterone using solid dispersions, inclusion complexes and micellar solubilization. Current Drug Delivery 2018;15(1):110-121.

17- Da Silva AC, de Freitas Santos PD, do Prado Silva JT, Leimann FV, Bracht L, Goncalves OH. Impact of curcumin nanoformulation on its antimicrobial activity. Trends in Food Science & Technology 2018;72:74-82.

18- Clinical and Laboratory Standards Institute. Performance Standards for Antimicrobial Susceptibility Testing. 30th ed. CLSI 2020, supplement M100 Wayne, PA.

19- Jain S, Bhanjana G, Heydarifard S, Dilbaghi N, Nazhad MM, Kumar V, et al. **Q4** Enhanced antibacterial profile of nanoparticle impregnated cellulose foam filter paper for drinking water filtration. Carbohydrate polymers 2018;202:219-226.

20- Jaiswal S, and Mishra P. Antimicrobial and antibiofilm activity of curcumin-silver nanoparticles with improved stability and selective toxicity to bacteria over mammalian cells. Medical Microbiology and Immunology 2018;207(1):39-53.

21- Hetta HF, Al-Kadmy I, Khazaal SS, Abbas S, Suhail A, El-Mokhtar MA, et al. Antibiofilm and antivirulence potential of silver nanoparticles against multidrug-resistant Acinetobacter baumannii. Scientific reports 2021;11(1):1-11.

22- Mosmann T. Rapid colorimetric assay for cellular growth and survival: application to proliferation and cytotoxicity assays. Journal of immunological methods 1983;65(1-2):55-63.

23- Abd-El-Aziz A, El-Ghezlani E, Elaasser M, Afifi T, Okasha R. First example of cationic cyclopentadienyliron based chromene complexes and polymers: synthesis, characterization, and biological applications. Journal of Inorganic and Organometallic Polymers and Materials 2020;30(1):131-146.

24- Gebreel RM, Edris NA, Elmofty HM, Tadros MI, El-Nabarawi MA, Hassan DH. Development and characterization of PLGA nanoparticle-laden hydrogels for sustained ocular delivery of norfloxacin in the treatment of Pseudomonas keratitis: an experimental study. Drug Design, Development and Therapy 2021;15:399.

25- Mekkawy AI, El-Mokhtar MA, Nafady NA, Yousef N, Hamad MA, El-Shanawany SM, et al. In vitro and in vivo evaluation of biologically synthesized silver nanoparticles for topical applications: effect of surface

coating and loading into hydrogels. International journal of nanomedicine 2017;12:759.

26- Paul S, Singh AR, Sasikumar CS. Green synthesis of bio-silver nanoparticles by Parmelia perlata, Ganoderma lucidum and Phellinus igniarius & their fields of application. Indian Journal of Research in Pharmacy and Biotechnology 2015;3(2):100.

27- Escárcega-González CE, Garza-Cervantes JA, Vazquez-Rodríguez A, Montelongo-peralta LZ, Treviño-Gonzàlez MT, Castro EDB, et al. In vivo antimicrobial activity of silver nanoparticles produced via a green chemistry synthesis using Acacia rigidula as a reducing and capping agent. International journal of nanomedicine 2018;13:2349.

28- Attallah NG, Elekhnawy E, Negm WA, Hussein IA, Mokhtar FA, Al-Fakhrany OM. In vivo and in vitro antimicrobial activity of biogenic silver nanoparticles against Staphylococcus aureus clinical isolates. Pharmaceuticals 2022;15(2):194.

29- Pal S, Tak YK, Song JM. Does the antibacterial activity of silver nanoparticles depend on the shape of the nanoparticle? A study of the gram-negative bacterium Escherichia coli. Applied and environmental microbiology 2007;73(6):1712-1720.

30- Bhuvaneswari T, Thiyagarajan M, Geetha N, Venkatachalam P. Bioactive compound loaded stable silver nanoparticle synthesis from microwave irradiated aqueous extracellular leaf extracts of Naringi crenulata and its wound healing activity in experimental rat model. Acta Tropica 2014;135:55-61.

31- Jain S, and Mehata MS. Medicinal plant leaf extract and pure flavonoid mediated green synthesis of silver nanoparticles and their enhanced antibacterial property. Scientific reports 2017;7(1):15867.

32- PAREI F, Ibrahim R, Nawas T. Antibacterial activity of curcumin against Lebanese clinical isolates of Staphylococcus aureus. MOJ Toxicol 2018;4(2):81-83.

33- Ali K, Ahmed B, Dwivedi S, Saquib Q, Al-Khedhairy AA, Musarrat J. Microwave accelerated green synthesis of stable silver nanoparticles with Eucalyptus globulus leaf extract and their antibacterial and antibiofilm activity on clinical isolates. PloS one 2015;10(7):e0131178.

34- Ansari MA, and Alzohairy MA. One-pot facile green synthesis of silver nanoparticles using seed extract of Phoenix dactylifera and their bactericidal potential against MRSA. Evidence-Based Complementary and Alternative Medicine 2018;2018.

35- Cardozo VF, Oliveira AG, Nishio EK, Perugini MRE, Andrade CGT, Silveira WD, et al. Antibacterial activity of extracellular compounds produced by a Pseudomonas strain against methicillin-resistant Staphylococcus aureus (MRSA) strains. Annals of clinical microbiology and antimicrobials 2013;12(1):1-8.

36- Morones JR, Elechiguerra JL, Camacho A, Holt K, Kouri JB, Ramírez JT, et al. The bactericidal effect of silver nanoparticles. Nanotechnology 2005;16(10):2346.

37- Farouk MM, El-Molla A, Salib FA, Soliman YA, Shaalan M. The role of silver nanoparticles in a treatment approach for multidrug-resistant Salmonella species isolates. International Journal of Nanomedicine 2020:6993-7011.

38- Bastos V, de Oliveira JF, Brown D, Jonhston H, Malheiro E, Daniel-da-Silva AL, et al. The influence of Citrate or PEG coating on silver

nanoparticle toxicity to a human keratinocyte cell line. Toxicology letters 2016;249:29-41.

39- Sahariah P, Sørensen KK, Hjálmarsdóttir MÁ, Sigurjónsson ÓE, Jensen KJ, Másson M, et al. Antimicrobial peptide shows enhanced activity and reduced toxicity upon grafting to chitosan polymers. Chemical communications 2015;51(58):11611-11614.

40- Gupta A, Briffa SM, Swingler S, Gibson H, Kannappan V, Adamus G, et al. Synthesis of silver nanoparticles using curcumin-cyclodextrins loaded into bacterial cellulose-based hydrogels for wound dressing applications. Biomacromolecules 2020;21(5):1802-1811.